JOURNAL OF MATERIALS SCIENCE 29 (1994) 4487–4499

Preparation of ceramic coatings from pre-ceramic precursors

Part I *SiC and "Si_3N_4/Si_2N_2O" coatings on alumina substrates*

M. R. MUCALO*, N. B. MILESTONE
Materials Science and Performance Group, The New Zealand Institute for Industrial Research and Development (Industrial Research Ltd), P.O. Box 31-310, Lower Hutt, New Zealand

I. C. VICKRIDGE
Institute of Geological and Nuclear Sciences, P.O. Box 31-312, Lower Hutt, New Zealand

M. V. SWAIN
CSIRO Division of Applied Physics, P.O. Box 218, Lindfield, NSW 2070, Australia

Scanning electron microscopy (SEM) and energy dispersive X-ray analysis (EDX) has indicated that adherent crack-free coatings of amorphous SiC and "Si_3N_4/Si_2N_2O" can be built up on planar alumina substrates by pyrolysis of layers of polycarbosilane (PCS) and poly(diphenyl)silazane (PDPS) precursors applied by spin- or dip-coating methods. In general, multilayers of black SiC can be prepared by pyrolysis of PCS layers at 1100 °C in a nitrogen atmosphere while transparent coatings consisting of multiple layers of Si_3N_4 are prepared by pyrolysis of either PCS or PDPS layers in a flowing atmosphere of ammonia at 1100 °C. The "Si_3N_4/Si_2N_2O" layers prepared by pyrolysing spin-coated layers of PDPS layers are found to be superior in quality (with respect to blemishes and embedded debris) than those prepared from spin-coated layers of PCS. Microhardness tests reveal that the coatings derived from PCS and PDPS are significantly softer than would be expected for SiC and Si_3N_4. X-ray photoelectron studies reveal that the surface of the PCS-derived SiC coatings consists of an SiO_2 layer while the surface of the PDPS-derived "Si_3N_4/Si_2N_2O" coating consists of an oxygen-rich silicon oxycarbonitride. These results are also generally supported by Rutherford backscattering spectra which also indicate considerable phase mixing of silicon, carbon, oxygen and nitrogen components within the bulk of the SiC and "Si_3N_4/Si_2N_2O" coatings on alumina.

1. Introduction

The formation of ceramics such as SiC and Si_3N_4 from organosilicon precursors is now well documented [1, 2]. Yajima *et al.* [3] pioneered the process of forming continuous SiC fibres by pyrolysis of polycarbosilane precursors in the 1970s. Owing to their distinct advantage of processability (namely solubility and fusibility), the polymeric organosilicon precursors find application in many areas such as fillers, bulk shapes, fibres or coatings which can be subsequently pyrolysed to form the desired ceramic articles [4]. Ceramic coatings, in particular, are of potential value in industry as a means of providing wear and corrosion resistance for articles used in adverse environments. For example, graphitic fibres and composites may be subjected to pore infiltration and consequent surface coating by pre-ceramic polymers which, upon pyrolysis, give ceramics which provide protection from adverse thermal and oxidizing conditions effectively extending their range of applications [1, 5]. The coating of articles with organic precursors using simple techniques such as spin- or dip-coating followed by relatively low-temperature pyrolysis offers a more controlled, versatile and potentially more economical route to ceramic coatings than would be afforded by using sintering, chemical vapour deposition (CVD) and plasma-coating methods [1, 6, 7]. SiC ceramics are also being considered as substitute substrates for silicon in the electronics industry [8], thus the formation of SiC coatings with desirable chemical, physical and electrical properties may find application in this area.

There are few detailed reports dealing with the preparation of ceramic coatings from pyrolysis of

* Author to whom all correspondence should be addressed. *Present address*: STA Fellow, Government Industrial Research Institute, Nagoya 1-1 Hirate-cho, Kita-ku, Nagoya City, Aichi Pref. 462, Japan.

0022–2461

organic precursors on planar substrates with most studies concerned with the application of ceramic coatings to fibres [4, 5, 9]. Si_2N_2O films have been the subject of research by previous investigators as replacements for silicon oxide films used as insulators for tunnel metal–insulator–silicon (MIS) diodes in transparent metal-type MIS solar cells [10]. This paper primarily describes the preparation of SiC and "Si_3N_4/Si_2N_2O" coatings formed by pyrolysis of layers of polycarbosilane and polysilazane precursors applied to planar alumina, silicon and silica glass substrates by spin- and dip-coating methods. SEM/EDX has been used to quantify deposition of ceramic material and examine coating quality, while X-ray photoelectron spectroscopy (XPS) and Rutherford backscattering (RBS) were employed to probe the surface and bulk characteristics of the coatings. Detailed characterization by infrared (i.r.), nuclear magnetic resonance (NMR) and X-ray diffraction (XRD) of the polycarbosilane and polysilazane precursors used in this study, as well as the residues obtained by pyrolysis, have been reported in a separate publication [11]. The mechanical properties of the coatings formed in this study were also assessed to test their suitability for use in abrasion resistance.

2. Experimental procedure

2.1. Preparation of pre-ceramic polymers

Poly(dimethyl)silane (PDMS) powder was prepared following the procedure described by Yajima *et al.* [3]. PDMS was subsequently converted [11] to the polycarbosilane (PCS) precursor to SiC by thermolysing 5–10 g of the white powder under argon in a silica glass-lined 100 ml capacity stainless steel bomb for 14–16 h at 470 °C. After cooling, the viscous yellow semi-glassy liquid left in the sleeve was dissolved in warm BDH Spectrosol hexane and subsequently filtered to produce a clear yellow liquid. Removal of the hexane under reduced pressure left a highly viscous yellowish liquid which could be used directly for coating without fractionation.

Poly(diphenyl)silazane (PDPS) was prepared as described previously [11] by the NH_4Br-catalysed polymerization of the oil obtained from ammonolysis of Ph_2SiCl_2. An additional NH_3 treatment of the polymer dissolved in ether was carried out to remove Si–Br bonds introduced during the polymerization in NH_4Br [12]. After filtration of the white solid produced, the ether was removed under reduced pressure leaving a flaky white material at the bottom of the flask which constituted PDPS.

2.2. Coating of substrates

PCS coating solutions 20%–70% (wt/vol) were prepared by dissolving pre-weighed amounts of PCS in measured volumes of *n*-hexane. PDPS coating solutions (40% (wt/vol)) were prepared by dissolving 0.40 g PDPS in 1 ml toluene.

Most data are reported for ceramic coatings on 99.5% Al_2O_3 plates. These were ultrasonically cleaned in a detergent solution for 5 min, rinsed in distilled water and then in A.R. acetone followed by drying. Clear fused quartz plates (silica, $\sim 15\,mm \times 15\,mm \times 3.2\,mm$) and polished, single-crystal silicon wafers (~ 0.4 mm thick) were also coated in this study.

Spin-coating was accomplished by placing a drop of coating solution on a plate contained in a stirrer pot attached to the shaft of a mechanical stirrer and then spinning (~ 6000 r.p.m. maximum rotation rate) to volatilize the solvent and spread the organic precursor over the plate. Dip-coating of substrates was carried out by using a d.c.-motor-driven lead screw arrangement which allowed immersion/withdrawal rates of 4–19 cm min^{-1}. Usually, an immersion/withdrawal rate of 4 cm min^{-1} was employed.

2.3. Pyrolyses

Pyrolyses of coated plates were conducted at 1100 °C in a temperature-programmed Pythagoras tube furnace under either flowing nitrogen (100 ml min^{-1}) or ammonia (200 ml min^{-1}) using heating rates of 120 °C h^{-1} (N_2) or 300 °C h^{-1} (NH_3) up to 1100 °C at which specimens were held for 2 h. The as-received or "wet" ammonia (Special Gases Division of New Zealand Industrial Gases Ltd) was found to contain 1250 p.p.m. water. "Wet" ammonia was dried by passing the gas through a column of KOH pellets and then through a column of anhydrous granular Na_2SO_4. Previous studies [11] demonstrated that the drying column significantly decreased the Si–O character in amorphous Si_3N_4 powders caused, in part, by the moisture present in the "wet" ammonia. However, coatings derived from pyrolysis of precursors in "wet" or "dry" ammonia showed no differences in appearance.

2.4. SEM/XRD/XPS/RBS instrumentation

Scanning electron micrographs and energy dispersive X-ray analyses (EDX) were recorded on a Cambridge Stereoscan 250 Mk II electron microscope employing a Link 860 Series 2 computing system. Samples examined were usually carbon-coated or gold–palladium-coated. EDX analyses of carbon-coated samples were conducted at 20 kV. X-ray diffraction patterns were acquired using a Philips PD1700 APD system employing a diffracted beam monochromator, automatic divergence slit and CoK_α radiation. Acquisition of X-ray photoelectron spectra was carried out using a Kratos XSAM 800 X-ray Photoelectron Spectrometer using a DS800 data system. Wide scans from 0–900 eV and over narrower energy windows were obtained using non-monochromatized MgK_α radiation of samples attached to stainless steel sample stubs by means of double-sided sticky tape. Spectra were usually referenced to the C 1s peak (284.8 eV) [13] due to the layer of adventitious hydrocarbons on samples. Sputtering was carried out by bombarding samples with 3 kV argon ions using an argon gas pressure of $\sim 10^{-8}$ torr (1 torr = 133.322 Pa) in the sample chamber. Curve-fitting an experimental Si 2p and O 1s profiles was carried out using Shirley baselines and 90% Gaussian/10% Lorentzian component

peaks. Rutherford backscattering spectrometry (RBS) was carried out on coated and uncoated samples in the new ion beam analysis (IBA) facility at the Institute of Geological and Nuclear Sciences Ltd. In typical experiments, 5–30 μC 2.0 MeV $^4He^+$ was incident on the samples in a 2 mm diameter beamspot with a current of 40–50 nA, and the elastically scattered α-particles were detected at 165°. Spectra were interpreted by fitting with RUMP [14] using assumed concentration profiles. This procedure does not necessarily give a unique sample structure for a given RBS spectrum, and so the elemental concentrations derived from these fits are tentative. The roughness of the substrate/coating interface was found to influence strongly the shape of the RBS spectrum. Although mixing of the coating and the substrate due to interdiffusion or solid-state chemical reactions would have a similar effect on the RBS spectrum, it is believed that in these samples the interfacial roughness is the dominant effect. This substrate roughness was approximated by using the "Fuzz" [15] mode in RUMP which superimposes a number of simulations, each of which assumes a different thickness of the coating.

2.5. Measurement of mechanical properties

2.5.1. Abrasion resistance

Abrasion resistance of the SiC and "Si_3N_4/Si_2N_2O" coatings was tested using a modified version of the Australian Standard AS 1774.23 by the Refractories Centre, CSIRO, Melbourne, Australia. The modifications to AS 1774.23 were that brown fused alumina grit having particle sizes between 180 and 425 μm was used as an erodent. In addition, the sample mask used in the test chamber was considerably reduced in size to cater for the small dimensions of the samples to be tested, i.e. a sample area of 15 mm × 15 mm was exposed to abrasion. Each plate tested was coated with four layers of SiC or "Si_3N_4/Si_2N_2O" which had been deposited by pyrolyses of spin-coated layers of PCS or PDPS. An uncoated AlSiMag plate (see later for compositional analysis of plates) was also subjected to the abrasion resistance test as a control specimen.

2.5.2. Microhardness

Microhardness measurements on coatings were carried out using the UMIS-2000, an ultra-microindentation system capable of applying extremely low loads in hardness measurements which was developed at the CSIRO Division of Applied Physics in New South Wales, Australia [16, 17].

Microhardness measurements were made on alumina plates coated with four layers of amorphous SiC and "Si_3N_4/Si_2N_2O" which had been applied by spin-coating layers of PCS and PDPS, respectively, followed by 1100 °C pyrolyses in nitrogen. Load–unload plots were obtained using loads of 500, 200, 100, 50, 20, 10 and 5 mN. Typically, at least six tests were done for each load at selected sites throughout the surface. A triangular diamond pyramid Berkovich-type indentor was used to make the indentations. The higher load indentations were examined using SEM in order to gain an insight into the adhesive and delamination performance of the coating under investigation. Microhardness measurements were also carried out on an uncoated alumina plate to obtain a value for the substrate hardness. Usually, the averaged data from load–unload plots were analysed.

3. Results and discussion

3.1. Spectroscopic characterisation of precursors and pyrolysis residues

A full description of the spectroscopic characterization of the precursors used in this study are given in a separate publication [11]. In general, infrared and NMR (^1H, ^{13}C, ^{29}Si) spectra of the PCS prepared for coating studies confirmed it to be identical to PC-470, one of the polycarbosilanes prepared by Yajima *et al.* [3]. NMR indicates that the PCS polymer skeleton consists of 50% SiC_4-type groups (i.e. $-[CH_2Si(CH_3)_2CH_2]-$) and 50% SiC_3H-type groups (i.e. $-[CH_2SiH(CH_3)_2CH_2]-$).

The infrared spectrum of PDPS [11], besides being dominated by vibrations associated with the phenyl group, indicates that NH and to a much lesser extent NH_2 groups are present in the solid polymer. The aromatic proton signal in the ^1H liquid NMR spectrum of the Ph_2SiCl_2-derived silazane broadens dramatically after NH_4Br-catalysed polymerization, confirming the polymeric nature of the product [11].

3.2. X-ray diffraction and solid-state NMR studies of 1100 °C pyrolysis residues

The XRD patterns of the ceramic residues obtained from pyrolysis of the PCS and PDPS at 1100 °C in either nitrogen or ammonia were generally broad and weak indicating the amorphous nature of the pyrolysis products. Coatings of SiC and "Si_3N_4/Si_2N_2O" reported in this study are generated by pyrolysis of the organosilicon precursors at 1100 °C, thus the coatings are likely to be composed of amorphous material. Combined XRD and ^{29}Si MAS NMR studies [11] demonstrated that the black material generated by pyrolysis of PCS in nitrogen was predominantly amorphous SiC. The "Si_3N_4/Si_2N_2O" comprising the PDPS-derived coatings is probably a complex amorphous silicon oxycarbonitride ($Si_xN_yO_zC_a$) on the basis of earlier ^{29}Si MAS NMR, XRD and mass-spectral studies of bulk residues from amorphous (and crystallized) residues from 1100 °C-NH_3 pyrolyses of PDPS and other SiC and Si_3N_4 polymeric precursors [11]. The PDPS-derived 1100 °C-NH_3 amorphous residue crystallizes at 1550 °C to produce a mixture of Si_3N_4 and Si_2N_2O hence the coatings on alumina plates are referred to as "Si_3N_4/Si_2N_2O" coatings.

3.3. Suitability of pre-ceramic polymers for coating: criteria

The most desirable property that a pre-ceramic polymer can have for coating is solubility in volatile organic solvents (e.g. hexane or toluene). In this way,

application to the substrate is effected easily by dissolution in the suitable organic solvent followed by the dispersion of the polymer on the substrate by a dipping or coating method during which the organic solvent evaporates leaving an intact layer of polymer on the substrate. It is also important that the polymer remains (in the absence of organic solvent) stable when stored (in sealed vessels) for long periods of time in a highly viscous liquid form. For example, the oil derived from ammonolysis of H_2SiCl_2 [18] is unsuitable for coating because it sets to an insoluble glassy material on standing in sealed containers due to cross-linking within the polymer. A silazane oil derived from the condensation of $MeHSiCl_2$ in ethylenediamine (polymethylsilylethylenediamine (PMSED)) studied in our laboratories was also deemed unsuitable for coating purposes because: (a) it was extremely moisture-sensitive and (b) it gradually set to a highly viscous insoluble rubbery substance and eventually solidified after 20 days standing in a sealed vessel [11]. In general, PCS and PDPS are found to be suitable coating polymers. PCS is soluble in hexane whilst PDPS is soluble in toluene. PDPS as a solid possesses advantages in handling and storage over PCS which in the present work was in the form of a highly viscous oil, although it is available commercially as a solid.

3.4. SiC coatings

Fig. 1 illustrates scanning electron micrographs of silicon carbide coatings on alumina (AlSiMag) plates applied by dip-coating (4 cm min^{-1}) of the substrates in 60% (wt/vol) PCS/hexane solution. In Fig. 1a, the pebbly appearance of the alumina substrate seen under high magnification is still apparent when coated with one thin SiC layer. However, as more SiC layers are formed by continued dip-coating and pyrolysis of the same substrate, the increase in total thickness of the SiC layers becomes evident by the smoothing out of the pebbly alumina surface in micrographs (see Fig. 1b). The rationale for forming multiple SiC layers on alumina (either by spin-coating or dip-coating methods) is to build up thickness and to coat over micro-cracks formed on previously deposited SiC layers. The colour of the alumina plate with one SiC coat is light brown, but after four to five SiC coats, it becomes a shiny black. SEM reveals that the initial three layers of SiC on alumina are relatively crack-free and uniform but that fourth or fifth layers exhibit cracking and some micro-spalling which expose underlying SiC coats.

EDX could be used to monitor the accumulation of SiC layers on alumina substrates by following the increase of the SiK_α peak intensity relative to the AlK_α peak intensity. Fig. 2 represents a plot of (%Si/%Al) versus number of coatings of SiC formed which predictably shows an increase in thickness as SiC layers are accumulated on the surface. An approximate indication of the thickness of the SiC coatings on alumina may be made by measuring the electron energy, E_0, at which the underlying substrate AlK_α peak disappears. This value may be used in the range, R, equation described by Kanaya and Okayama [19] namely,

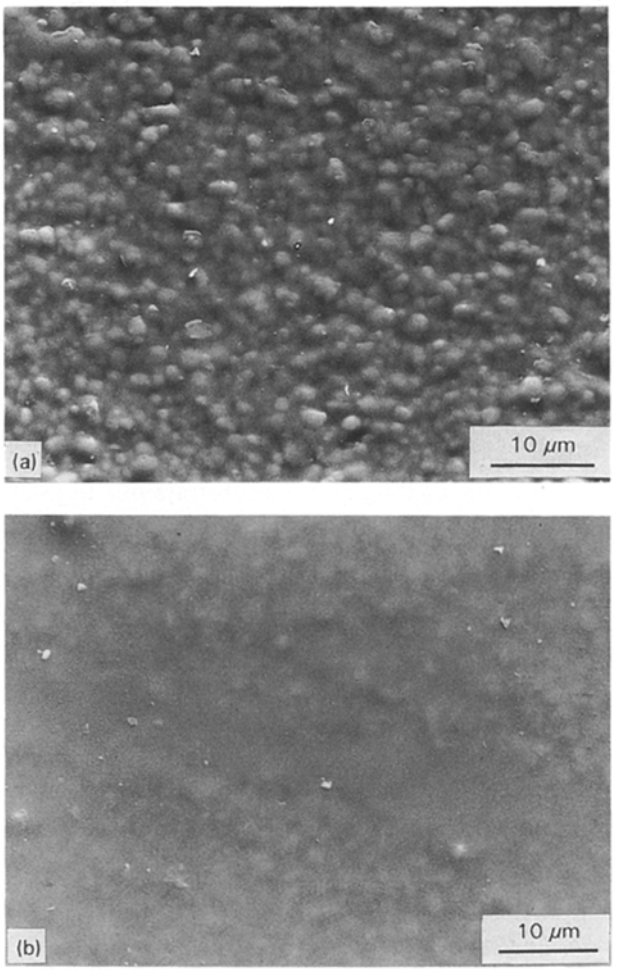

Figure 1 Scanning electron micrographs of SiC coatings on alumina plates deposited by a 2 h 1100 °C pyrolysis of plates dip-coated at 4 cm min^{-1} in 60% (wt/vol) PCS/hexane solution: (a) plate with one SiC layer, and (b) plate with three SiC layers.

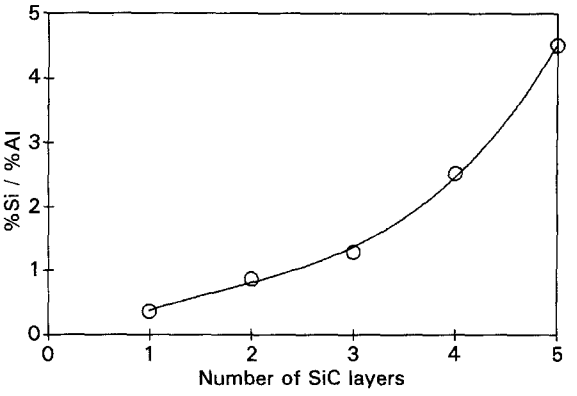

Figure 2 %Si/%Al versus the number of coatings of SiC for coatings applied by pyrolysis of spin-coated layers of PCS on an alumina plate (% = at %).

$R = 0.0276A/\rho Z^{8/9}(E_0^{5/3}-E_c^{5/3})$, where ρ is density (g cm^{-3}), A is relative atomic mass, Z is atomic number of the target, and E_c is the threshold electron energy below which X-rays emanating from the underlying alumina substrate would fail to escape from the sample (for aluminium, $E_c = 1.559$ kV). For SiC, a weighted value of $A/Z^{8/9}$ is given by the sum of the individual $A/Z^{8/9}$ values for silicon and carbon each multiplied, respectively, by the weight fraction, w_f,

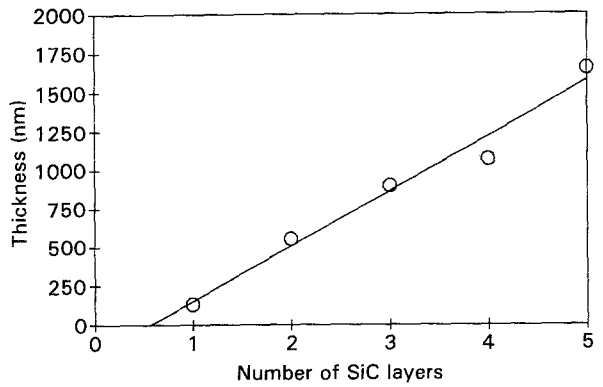

Figure 3 Calculated thickness versus number of layers for SiC coatings on alumina plates (derived from pyrolysis of spin-coated PCS).

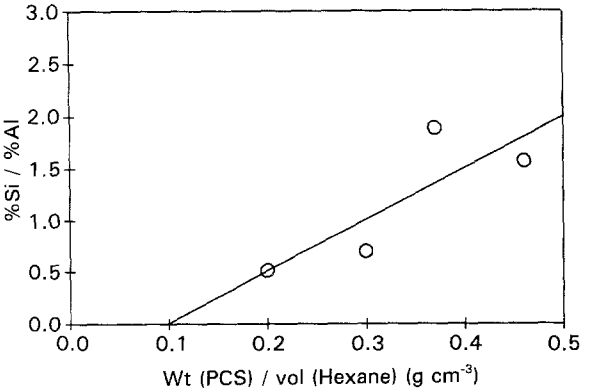

Figure 4 EDX-derived graph of %Si/%Al (for SiC coatings on alumina) versus wt/vol (weight of PCS added to volume, v, of hexane) values for PCS/hexane coating solutions. The PCS/hexane solutions of different wt/vol values were spin-coated on to the alumina plates (% = at %).

values of silicon and carbon in SiC. Thus $A/Z^{8/9}$ (SiC) is given by $\{[A/Z^{8/9}(\text{Si})\, w_f(\text{Si in SiC})] + [A/Z^{8/9}(\text{C})\, w_f(\text{C in SiC})]\}$. For SiC, this yields a value of 2.61. A plot of SiC thickness calculated by this method versus the number of SiC layers is found to demonstrate reasonable linearity (see Fig. 3). Repeated application (up to 5) of thin spin-coated PCS (followed by a complete firing after each application) to the same substrate leads to hard, black adherent SiC coatings of ~ 2 μm thickness while SiC coatings formed from repeated dip-coating of the same substrate using identical firing conditions are thinner (~ 1 μm for four layers).

The quality and adherency of the SiC coatings is determined by the concentration of the PCS/hexane coating solution and the coating method. In this study, EDX analyses on the single SiC layers derived from spin-coating 10%–45% (wt/vol) PCS/hexane coating solutions on alumina indicate that the quantity of SiC deposited (expressed as (%Si/%Al)) increases in an approximately linear fashion with per cent wt/vol values (see Fig. 4). However, SiC coatings derived from PCS/hexane coating solutions $> 45\%$ (wt/vol) are spalled and severely cracked. When dip-coating (at 4 cm min^{-1}) is employed, considerably less PCS is applied to the substrate and coating solutions of twice the concentration can be used (i.e. 60%–70% (wt/vol)). Concentrations for coating solutions will tend to be unique for the particular precursor involved, because various organosilicon precursors can give significantly different ceramic yields thus determining the amount of coating material left on the plate after pyrolysis.

The SiC coatings obtained from dip-coating appear generally somewhat streaked due perhaps to the withdrawal process of the plate from the coating solution. Improvement in coating quality is afforded by passing the arm holding the specimens through a Teflon guide which absorbs vibrations caused by the travel of the lead-screw. Dip-coating offers advantages over spin-coating in that non-planar objects may be coated. However, despite the fact that spin-coating is restricted to planar objects, it is found that coating thickness and quality are higher. Fig. 5 illustrates alumina plates coated with multiple layers of SiC by spin- and dip-coating methods. Adherent, uniform and relatively crack-free SiC coatings can also be formed on silica glass and silicon wafers using spin- and dip-coating techniques.

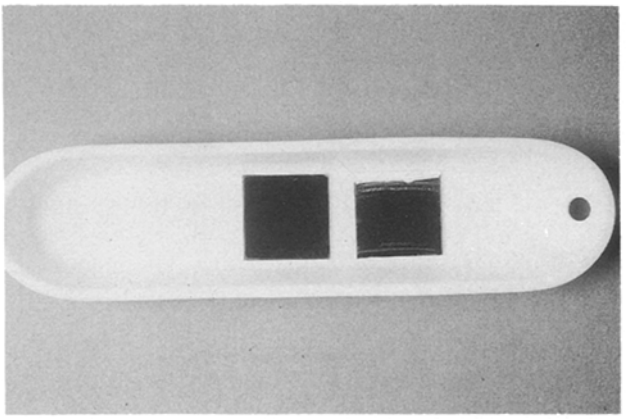

Figure 5 Photograph comparing SiC coatings on alumina generated by spin- or dip-coating methods: left, plate with five SiC layers applied by spin-coating of PCS/hexane solutions on to the substrate, and right, plate with four SiC layers applied by dip-coating of the substrate into PCS/hexane coating solutions.

Pyrolytic silicon carbide (i.e. β-SiC) has a relatively low thermal expansion coefficient, α, of 4.4–4.6 $\times 10^{-6}\,°\text{C}^{-1}$ over the temperature range 20–1000 °C [20] while for silicon and clear fused quartz, α is $\sim 2.6 \times 10^{-6}$ and $0.55 \times 10^{-6}\,°\text{C}^{-1}$, respectively [21, 22]. The partial matching of these low thermal expansion coefficient materials may explain the success of forming adherent, relatively crack-free multilayers of SiC on silicon and silica substrates. For alumina, α falls in the range $7.7\text{–}9.0 \times 10^{-6}\,°\text{C}^{-1}$ [8] yet coatings of SiC may still be successfully formed on alumina plates. It is possible that chemical interactions of the PCS with the aluminium oxide substrate via the SiH group (at which cross-linking of the polymer is known to occur) may play an important role in determining coating quality and adherency. Indeed, studies [22] following the formation of SiC films from various alkylsilane/hydrogen or chloroalkylsilane/hydrogen mixtures on alumina substrates by CVD indicate that Si–O–Al interactions can occur.

3.5. "Si_3N_4/Si_2N_2O" coatings

"Si_3N_4/Si_2N_2O" coats were obtained by pyrolysis of layers of PCS and PDPS applied to alumina plates by spin- and dip-coating methods.

3.5.1. "Si_3N_4/Si_2N_2O" coatings derived from PCS

Fig. 6a is a low magnification micrograph of an alumina plate with two coatings of transparent material formed by pyrolyses in ammonia at 1100 °C of PCS applied to the substrate by spin-coating. At low magnification, it is difficult to deduce whether a coating exists on the pebbly alumina substrate. The surfaces of the substrates studied (Si/Al_2O_3) tended to be littered with apparent debris which in a high-magnification SEM (Fig. 6b) were found to be part of the coating itself. The embedded fibres and craters constitute imperfections in the coating and are possibly caused by bubbling of the polymer during the pyrolysis process in ammonia.

3.5.2. "Si_3N_4/Si_2N_2O" coatings derived from PDPS

Fig. 7a–f is a series of scanning electron micrographs which illustrate the build-up of PDPS-derived "Si_3N_4/Si_2N_2O" on alumina plates. The increase in thickness of the coating on the alumina plate is clearly demonstrated by the virtual "smoothing out" of the pebbly surface associated with the alumina substrate. In the first two coatings on the plates, some small fissures in the "Si_3N_4/Si_2N_2O" layers are evident (see Fig. 7b and c) however, these disappear or are coated over by the third, fourth and fifth coatings. As coating thickness builds up, the PDPS-derived "Si_3N_4/Si_2N_2O" coatings gradually take on a sheen which, by the second or third coating, exhibit a slight degree of interference colours. The PDPS-derived "Si_3N_4/Si_2N_2O" coatings are also generally free of the embedded debris which was a typical characteristic of the PCS-derived "Si_3N_4/Si_2N_2O" coatings (cf. Fig. 6).

Alumina plates with one to six layers of PDPS-derived "Si_3N_4/Si_2N_2O" were prepared and carbon-coated for EDX examination. Fig. 8 is a plot of (%Si/%Al) versus the number of "Si_3N_4/Si_2N_2O" coatings. It is apparent that the amount of coating material on the alumina plate surface increases in an approximately linear fashion as the number of layers applied increases. The range equation (see earlier) used for determining SiC thicknesses was once again employed in this system for determining approximate "Si_3N_4/Si_2N_2O" thicknesses. Separate calculations of the thickness were performed using weighted $A/Z^{8/9}$ values for Si_3N_4 and for Si_2N_2O. However, because the thicknesses calculated on the basis of 100% Si_2N_2O and 100% Si_3N_4 coatings were not very different in magnitude, an average of the two thicknesses was computed and plotted versus the number of applied layers in Fig. 9. In general, "Si_3N_4/Si_2N_2O" coatings of ~ 1 μm thickness can be prepared corresponding to the deposition of five layers of "Si_3N_4/Si_2N_2O" by pyrolysis (in ammonia) of PDPS

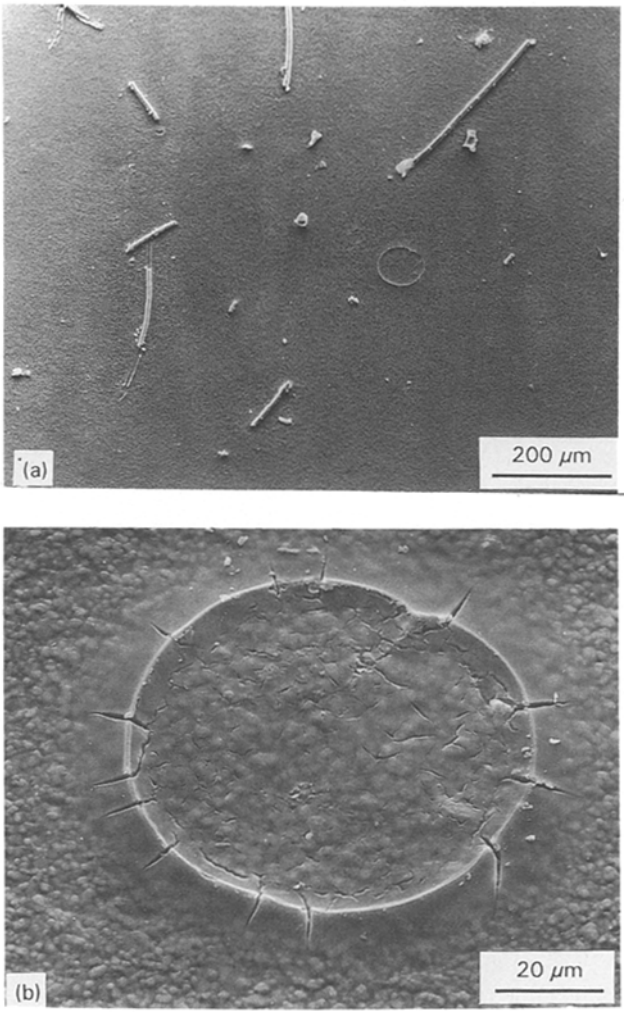

Figure 6 "Si_3N_4/Si_2N_2O" layers on an alumina plate applied by the 1100 °C pyrolysis in ammonia of PCS layers applied by spin-coating: (a) lower magnification micrograph demonstrating the debris littering the surface of the coating, and (b) higher magnification micrograph illustrating embedded fibres.

layers spin-coated onto the substrate from a toluene solution. In Fig. 9, the plot of "Si_3N_4/Si_2N_2O" thickness versus the number of "Si_3N_4/Si_2N_2O" layers is slightly non-linear in that a large increase in thickness is observed after application of the second "Si_3N_4/Si_2N_2O" layer. This may suggest some non-uniformities in areas of the coating.

Si_3N_4 (hot-pressed or reaction-sintered) has a slightly lower thermal expansion coefficient ($3.31 \times 10^{-6}\,°C^{-1}$ from 21–1315 °C [23]) than pyrolytic SiC (see earlier). In the present study, "Si_3N_4/Si_2N_2O" coatings were generally only formed on alumina substrates. The coatings of amorphous "Si_3N_4/Si_2N_2O" successfully formed on alumina plates do so for similar reasons contributing to the success in forming SiC coatings on alumina, i.e. Al–O–Si interactions (see earlier).

3.6. X-ray photoelectron spectra of the coatings

3.6.1. PCS-derived SiC coatings

Initial examination of the black SiC coatings by XPS reveals silicon, carbon and oxygen to be present on the

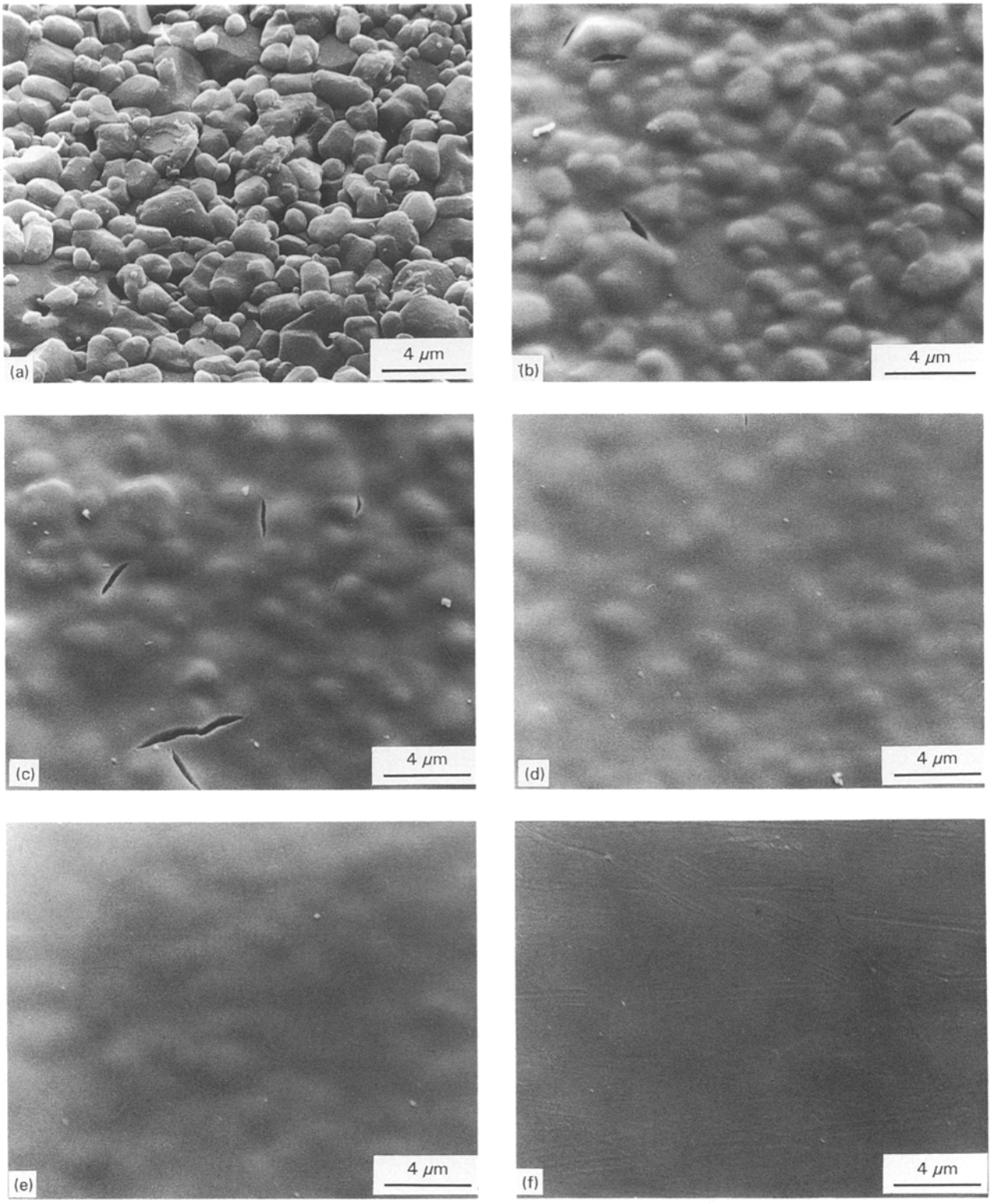

Figure 7 Scanning electron micrographs of uncoated and "Si_3N_4/Si_2N_2O"-coated alumina plates produced by pyrolysing spin-coated PDPS in dried ammonia: (a) uncoated alumina plate, (b) one layer of "Si_3N_4/Si_2N_2O", (c) two layers, (d) three layers, (e) four layers and (f) five layers.

surface. The O 1s peak is particularly strong and a quantitative analysis of the surface components showed that the Si:O ratio was $\sim 1:2$ suggesting that SiO_2 is a major surface species on the SiC coating. This was confirmed from the binding energy position of the Si 2p peak (103.53 eV) which is typical for SiO_2 [13]. A 15 min argon ion sputter was carried out to ascertain whether the SiO_2 layer was of sufficient thinness to be etched away. The X-ray photoelectron spectrum of the sputtered coating is shown in Fig. 10. After sputtering, the O 1s peak remained relatively unchanged; a quantitative analysis revealed the Si:O ratio to be largely unchanged at 1:1.9. However, the C 1s peak had almost disappeared (see Fig. 10) which showed that the carbon originally detected was associated with adventitious hydrocarbons and not with carbide in the SiC coating. A further 30 min sputtering produced no change in the X-ray photoelectron spectrum thus indicating that the SiO_2 layer existing on the PCS-derived SiC coating is of significant thick-

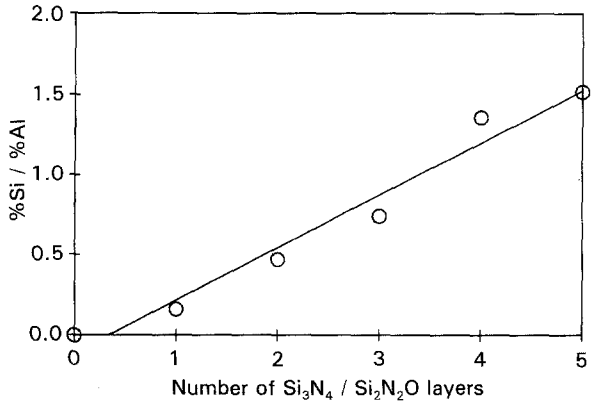

Figure 8 EDX-derived graph of %Si/%Al (for "Si_3N_4/Si_2N_2O" coatings on alumina) versus the number of layers of PDPS-derived "Si_3N_4/Si_2N_2O" on alumina plates (% = at %).

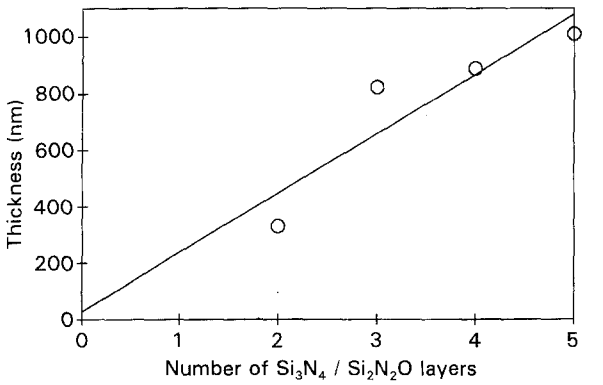

Figure 9 Calculated thickness versus the number of layers for "Si_3N_4/Si_2N_2O" coatings on alumina plates. Thickness values derived from calculations using weighted $A/Z^{8/9}$ values for Si_3N_4 and Si_2N_2O have been averaged.

ness. Earlier ^{29}Si MAS NMR studies [11] showed no Si–O character in the black amorphous residues derived from 1100 °C-N_2 pyrolysis of PCS so that the Si–O character is not a characteristic of the bulk material. It is possible that PCS-derived amorphous materials develop a protective skin of SiO_2 upon exposure to an ambient atmosphere. Schreck *et al.* [24] found, from X-ray photoelectron spectroscopy of Nicalon NML 202 SiC fibres, that the entire surface spectrum of the industrially produced fibre corresponds to SiO_2, which can form by deliberate exposure of the PCS fibre to oxygen during manufacture. In this study, the PCS-derived SiC coatings were not pyrolysed under oxygen at any stage, thus it is likely that the surfaces of the coatings may become oxidized under ambient conditions immediately after being taken out of the furnace or on standing for a long period of time. The formation of SiO_2 on such coatings appears to be independent of the substrate as surfaces of PCS-derived SiC coatings formed at pyrolysis temperatures of 700–800 °C on stainless steel and mild steel plates were also found to contain SiO_2 [25].

3.6.2. PDPS-derived "Si_3N_4/Si_2N_2O" coatings

When the transparent "Si_3N_4/Si_2N_2O" coatings on alumina were first examined by XPS, N 1s (in addition to Si 2p, Si 2s, C 1s and O 1s) is detected on the surface. The binding energy position (397.98 eV) of

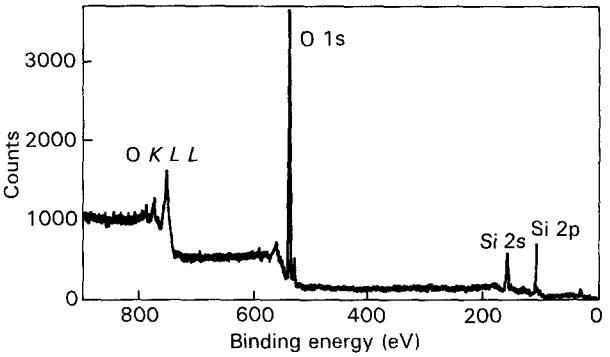

Figure 10 X-ray photoelectron spectrum of a PCS-derived SiC coating (five layers applied by spin-coating and 1100 °C-N_2 pyrolysis) on an alumina plate after 15 min argon ion sputtering.

N 1s confirms the peak to be representative of a nitride species [26]. Thus, unlike the SiC coatings where carbide-associated carbon is obscured from XPS detection by a thick overlying layer of SiO_2, part of the nitride comprising the PDPS-derived coating is at the surface. However, the O 1s peak in the X-ray photoelectron spectrum of the PDPS-derived coating is intense (Si:O = 1:2.3) which indicated that the "Si_3N_4/Si_2N_2O" coatings exhibit a significant degree of surface oxidation.

Deconvoluting the broad Si 2p envelope obtained from a narrow scan over this region revealed three possible species which were contributing to the profile with shifts of 102.1, 102.75 and 103.31 eV and intensity ratios of 1:0.6:1. The peak at 103.31 eV is due to a SiO_2 species whilst the peaks at 102.1 and 102.75 eV could possibly be assigned to Si_3N_4 and Si_2N_2O type species, respectively.

Argon ion sputtering for 5 min decreased C 1s significantly while only slightly decreasing N 1s. In contrast, Si 2p and O 1s increased in intensity. Sputtering was continued over an extended period of time (~ 70 min) to monitor the change in the spectrum. The resultant spectrum is illustrated in Fig. 11. It was interesting to note that a weak C 1s signal persisted even after 70 min sputtering. The binding energy position of the C 1s peak was deduced to be ~ 284.0 eV (after correction of the Si 2p peak to the Si 2p peak position in the spectrum acquired before sputtering) which suggests that the peak is representative of graphitic carbon [13]. This demonstrates that there is a small amount of carbon remaining in the coating after 1100 °C-NH_3 pyrolysis. The Si:N:C:O ratio as deduced from the quantitative analysis of the sputtered coating was found to be 1:0.30:0.18:1.79. The presence of carbon in the PDPS-derived coatings agrees with allied XRD/mass spectrometric studies [11] which demonstrated that white amorphous residues derived from 1100 °C-NH_3 pyrolyses of preceramic polymers consist of silicon oxy*carbo*nitrides.

3.7. Rutherford backscattering spectra of the coatings

3.7.1. PCS-derived SiC coatings

Fig. 12 shows the Rutherford backscattering spectrum of a SiC coating formed by spin-coating on an alum-

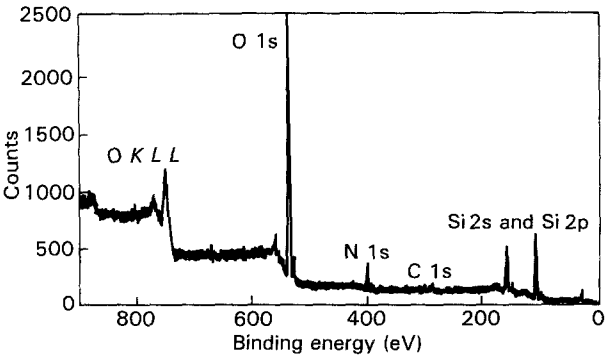

Figure 11 X-ray photoelectron spectrum of a PDPS-derived "Si_3N_4/Si_2N_2O" coating (four layers applied by spin-coating and 1100 °C-"dry" ammonia pyrolysis) on an alumina plate after 70 min argon ion sputtering.

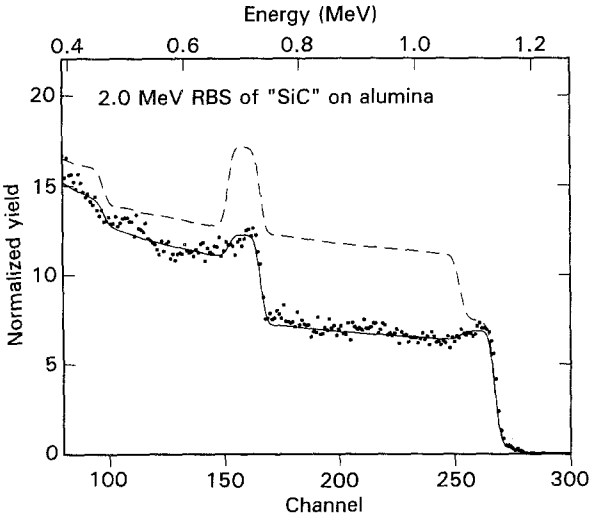

Figure 12 Rutherford backscattering spectrum of a PCS-derived SiC coating on alumina prepared by spin-coating (black dots) and RUMP-generated simulation spectra for (——) $SiO_{2.2}$ (180 nm)/SiCO (1600 nm)/Al_2O_3 (5000 nm) and (– – –) SiO_2 (180 nm)/SiC (1600 nm)/Al_2O_3 (5000 nm). "Fuzzing" over 500 nm in layer 2 and a straggling factor of 1 have been incorporated into both simulations.

ina substrate. The RUMP simulation curve which agrees most closely with the experimental profile is calculated assuming three layers consisting of (1) 180 nm $SiO_{2.2}$, (2) 1600 nm SiCO, and (3) 5000 nm (i.e. an infinitely thick layer) Al_2O_3. The appearance of the experimental RBS profile also suggests a gradual compositional transition from the first layer to the second layer rather than a sharp change. The composition of the first simulated layer agrees well with XPS results described earlier which demonstrated the existence of an SiO_2 layer on the surface of the coatings. The composition of the second simulated layer is a little more surprising given that it describes the bulk of the coating which would be expected to consist predominantly of SiC. This is evident from a RUMP simulation for a coating consisting of 180 nm SiO_2 (layer 1) and 1600 nm SiC (layer 2) which shows that silicon in the second layer is overestimated if this coating layer composition is assumed (see Fig. 12). The fact that the RBS spectral profile of the SiC coatings indicates oxycarbide in the "second layer" of the coating suggests that phase mixing has occurred in the bulk of the coating. This may have occurred as a result of the preparation of multilayered coating. The synthesis of each PCS-derived ceramic layer has probably given rise to layers each with an oxidized (SiO_2) surface layer containing SiC in the bulk underneath. With the deposition of further layers and the consequent 1100 °C pyrolysis required each time a layer is formed, it is highly possible that phase mixing has occurred thus "blurring" demarcations between separately deposited layers.

3.7.2. PDPS-derived "Si_3N_4/Si_2N_2O" layers

The Rutherford backscattering spectrum for the PDPS-derived "Si_3N_4/Si_2N_2O" layers formed by spin-coating on alumina is shown in Fig. 13. It is evident from the superimposed solid line simulation spectrum (see Fig. 13) that these coatings also consist of two distinct layers with a considerable degree of phase mixing. The first layer (thickness 250 nm) in the simulation system has been tentatively assigned a composition of $SiO_{1.5}C_{0.5}N_{0.1}$ with the second layer (thickness 690 nm) being composed of $SiO_{1.2}C_{0.7}N_{0.5}$. The third layer in the simulation system was the "infinitely thick" (5000 nm) layer of alumina for the substrate. A relatively oxygen-rich and nitrogen-deficient primary layer is expected in this coating system on the basis of XPS results with relatively less oxygen and more nitrogen in the bulk of the coating. The dashed line simulation spectrum for a coating system consisting of 940 nm Si_2N_2O overlying an infinitely thick layer of Al_2O_3 (Fig. 13) clearly shows that the PDPS-derived coatings are nitrogen-deficient with respect to Si_2N_2O. Unlike the SiC/alumina system, the two layers detected in this coating system are slightly more distinct.

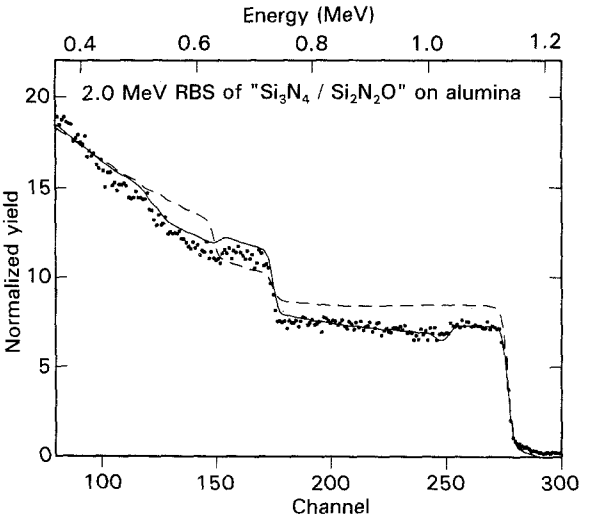

Figure 13 Rutherford backscattering spectrum of a PDPS-derived "Si_3N_4/Si_2N_2O" coating on alumina prepared by (●) spin-coating, and RUMP-generated simulation spectra for (——) $SiO_{1.5}C_{0.5}N_{0.1}$ (250 nm)/$SiO_{1.2}C_{0.7}N_{0.5}$ (690 nm)/Al_2O_3 (5000 nm) and (– – –) Si_2N_2O (940 nm)/Al_2O_3 (5000 nm). "Fuzzing" over 650 nm and a straggling factor of 1 have been incorporated into the simulation.

3.8. Measurement of mechanical properties

3.8.1. Abrasion resistance

The coatings were subjected to two types of abrasion resistance testing which gave rather different results. The first was a non-standard, informal test in which the coatings were simply scratched with a nickel spatula. The coatings were hard enough such that they could not be scratched when subjected to this test. Metal, in fact, was scratched off the spatula on to the coating.

In the second abrasion resistance test, the weight loss of specimens was used to gauge resistance to erosion. This was a standard abrasion resistance test as utilized in industry [23]. The results for the plates tested are summarized in Table I. Although, weight losses for all plates tested were small, they were very similar in magnitude. It was apparent that the polymer-derived SiC and "Si_3N_4/Si_2N_2O" coatings did give a very small amount of protection (at most $\sim 4.5\%$) against eventual erosion of the alumina substrate. This abrasion resistance test completely stripped off the SiC and "Si_3N_4/Si_2N_2O" coatings and had abraded some of the underlying substrate as well, thus part of the weight loss recorded is due to the weight of the removed coating. An estimate made of the contribution that the removed SiC or "Si_3N_4/Si_2N_2O" coating would make to the weight losses recorded, made the assumption that the coating was removed as a rectangular box (equal to the testing area) of volume $(15 \times 10^{-3} \times 15 \times 10^{-3} \times$ (thickness of coating)) m^3. For thicknesses of SiC and Si_3N_4/Si_2N_2O coatings, data were used from previous SEM studies for spin-coated plates, i.e. ~ 1161 nm for four layers of SiC and ~ 870 nm for four layers of "Si_3N_4/Si_2N_2O". An approximate mass of coating material removed could then be computed by multiplying the volume of each rectangular section removed by the density value assuming pure SiC and Si_3N_4. For SiC a density value of $3.21 \times 10^6\ g\,m^{-3}$ [19] was used while for Si_3N_4, $3.19 \times 10^6\ g\,m^{-3}$ [27] was used for density. The results of these computations are summarised in Table I. It is evident that the thin coating material makes a very small contribution to the overall weight loss (for Si_3N_4, $\sim 1.5\%$ and for SiC, $\sim 2.0\%$) so that the reduced weight loss demonstrated by the coated alumina plates after abrasion is due mostly to the protective action of the SiC and "Si_3N_4/Si_2N_2O" coatings.

3.8.2. Microhardness experiments

Conventional methods for measuring microhardness of materials have indentation loadings in the range 0.1–5 N and are thus limited to characterizing coatings $\gtrsim 3\ \mu m$ thick [16]. In the present study, the amorphous SiC and "Si_3N_4/Si_2N_2O" coatings on the alumina were considerably thinner which necessitated using an indentation instrument capable of producing much smaller indentation forces. The UMIS-2000 is designed to measure microhardness for thin coatings or near surface material. The elastic modulus, E, of the indented materials is calculated from the slope of the unloading curve at the peak load following the procedure proposed by Loubet *et al.* [28]. The hardness, H (GPa), derived from the UMIS-measurements is defined [15] by a relationship between depth and indentor load, P, i.e. $H = P/A$, where A is the area of contact given by $A = kh_p^2$ and h_p is the effective plastic depth of penetration which is also obtained from analysis of the unloading curve following the recent approach of Oliver and Pharr [29] and k is a geometric constant for the Berkovich indentor ($k = 24.5$).

Fig. 14 illustrates typical load–unload plots for the SiC-coated and "Si_3N_4/Si_2N_2O"-coated alumina plates for a load of 10 mN. The corresponding hardness, H, versus h_p (penetration) plots are shown in Fig. 15. Table II summarizes the hardness, effective modulus [16] and measured depth of penetration attained for each loading from 5–50 mN. In Fig. 15, there is a vertical marker on the x-axis which marks the depth below which the radius of the tip of the indentor interferes or compromises the analysis. Above this marker, the measured values of H exhibit a significantly lower rate of increase in effect almost levelling off. In Table II, hardnesses of the SiC coatings show some scatter in falling between 10.3 and 11.7 GPa but are generally independent of load. Coatings of "Si_3N_4/Si_2N_2O" are significantly softer than SiC coatings and show much less scatter in hardness values which range from 3.15–3.19 GPa for loads of 5–20 mN.

Although there is some consistency in hardness values of both SiC and "Si_3N_4/Si_2N_2O" coatings for the low loadings (5–50 mN), the values of effective modulus increasing with increasing depth of penetration (see Table II). This behaviour is typical for films that have materials of higher modulus as substrates. The general form of the load–unload curves is consistent with the fact that the SiC and "Si_3N_4/Si_2N_2O" coatings are soft coatings on harder substrates. Hard coatings on softer substrates (e.g. TiN on stainless steel) tend to give load–unload curves with a pronounced "knee" occurring at a certain penetration depth, the points below which represent the bulk coating material [16]. The softness of the SiC and "Si_3N_4/Si_2N_2O" coatings relative to alumina also agrees with the abrasion resistance results where ceramic layers were completely stripped from the alumina plates after being subjected to a stream of brown fused alumina. In the "Si_3N_4/Si_2N_2O"-coated alumina sample, the influence of the underlying substrate on measured microhardness appears obvious for a 50 mN indentation force which gives a significantly higher hardness value of 4.25 GPa for a penetration of 689 nm. This is not surprising, because the penetration depth is close in value to the expected thickness of the "Si_3N_4/Si_2N_2O" coating (~ 870 nm for four layers, see earlier). The effect of the substrate on the hardness value measured for four layers of SiC coated on alumina for a measured penetration of 514 nm (50 mN load) is less apparent as the thickness of PCS-derived SiC coatings is higher (~ 1160 nm, see earlier).

The indentations produced by the very low loads (e.g. 10 mN) on the UMIS-2000 are too small to be measured by optical methods as required in standard procedures for evaluating microhardness of materials

TABLE I Results of abrasion resistance testing (modified version of AS 1774.23) on uncoated, SiC-coated and "Si_3N_4/Si_2N_2O"-coated alumina plates

Sample tested	Weight loss (g)	Contribution[a] of coated material to weight loss (g)
Uncoated Al SiMag plate	0.0401	Not applicable
PCS-derived SiC-coated alumina plate	0.0389	0.0008
PDPS-derived "Si_3N_4/Si_2N_2O"-coated alumina plate	0.0383	0.0006[b]

[a] Computed (see text).
[b] The calculated weight loss is approximately the same if the density for either Si_3N_4 (3.19×10^6 g m^{-3}) or Si_2N_2O (3.10×10^6 g m^{-3}) is used.

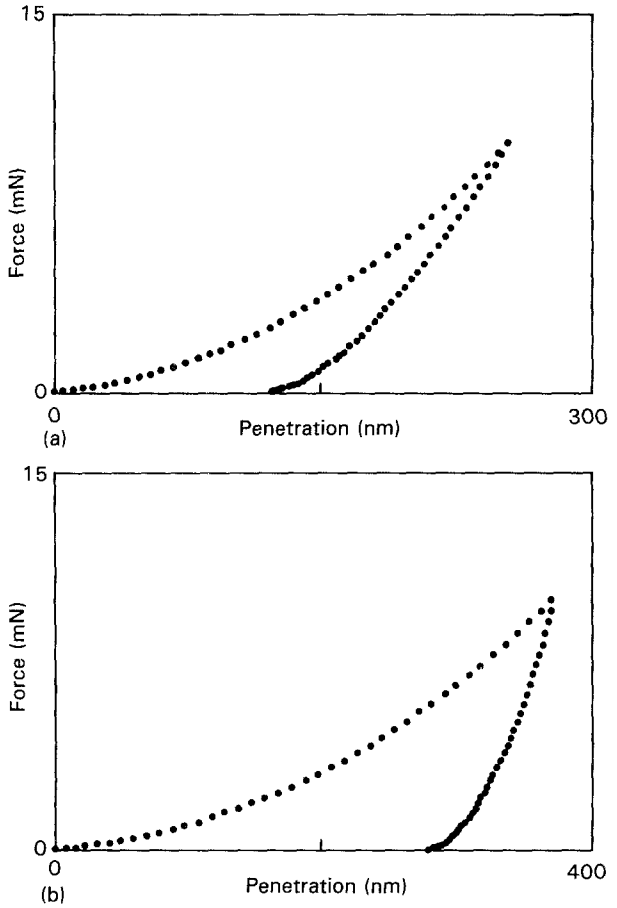

Figure 14 Load–unload curves for maximum applied force of 10 mN: (a) SiC-coated alumina (average curve for seven separate indentations) and (b) "Si_3N_4/Si_2N_2O"-coated alumina (average curve for eleven separate indentations).

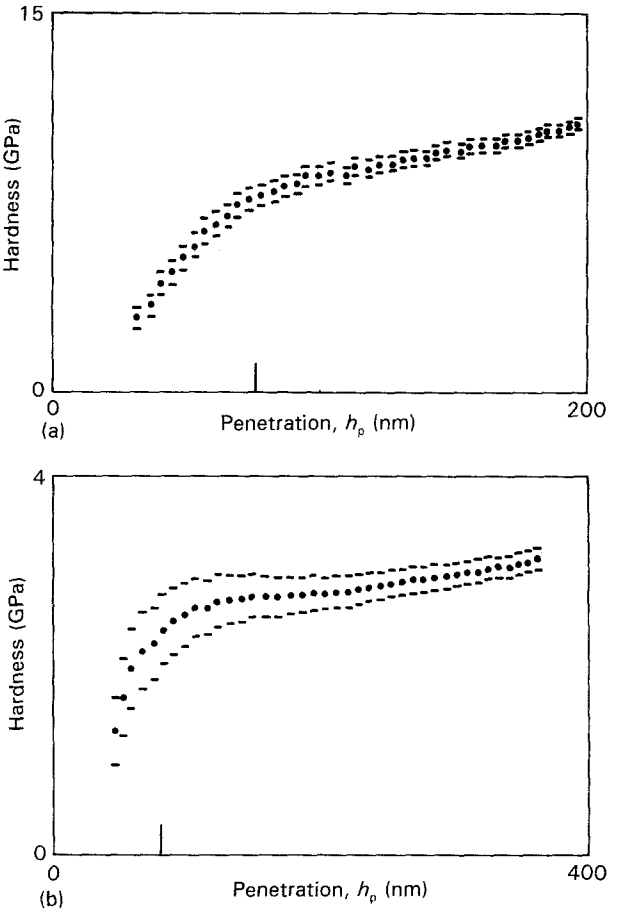

Figure 15 Hardness versus h_p (elastic/plastic penetration) for (a) SiC-coated alumina plate, and (b) "Si_3N_4/Si_2N_2O"-coated alumina plate. The standard deviation for each point is shown in the graph.

[16], thus it is not possible directly to equate hardness values to those obtained by other conventional methods. However, the UMIS-derived measurements are consistent with the general hardness trends of various materials. In the present study, the pre-ceramic polymer-derived SiC and "Si_3N_4/Si_2N_2O" coatings are significantly softer than the uncoated alumina substrate which gave UMIS-determined hardness values in the range 15–26 GPa. A range of hardness values was obtained because of the inherent roughness (pebbliness) of the alumina surface (compared to the smoother coated surfaces) which introduces non-reproducibility during indentation measurements. It is evident that the SiC and "Si_3N_4/Si_2N_2O" coatings on alumina are significantly softer than pure and crystalline SiC and Si_3N_4 which exhibit Vickers hardness values of 27–30 and 18–20 GPa, respectively. The UMIS-derived hardness values measured for the SiC on alumina coatings appear to agree more closely with Vickers hardness measurements performed on pyrolytic compacts of silicon carbonitrides which gave values of 9.5 GPa [30]. This means that strictly speaking the amorphous material comprising the coatings is not pure Si_3N_4 or SiC but complex compounds containing oxygen and carbon impurities which are influencing mechanical properties.

An SEM examination of the triangular-shaped depressions made by the Berkovich indentor in the coatings showed that the coating did not delaminate or crack in the vicinity of the indentation.

TABLE II Summary of microhardness measurements[a] performed by the UMIS-2000 on PCS-derived SiC and PDPS-derived "Si_3N_4/Si_2N_2O" coatings[b] on alumina plates

Specimen	Load (mN)	Hardness (GPa)	Modulus (GPa)	Max. measured penetration[c] (nm)
SiC coating on alumina	5	11.2	87	175
	10	10.6	96	253
	20	10.3	112.2	358
	50	11.7	161.5	514
"Si_3N_4/Si_2N_2O" coating on alumina	5	3.19	70.7	260
	10	3.15	95.2	369
	20	3.18	138.5	510
	50	4.25	320.8	689
Uncoated alumina substrate	50	22.0	404.0	376
	100	22.8	506.0	429
	200	16.8	331.0	754
	500	15.3	239.0	1306

[a] Measurements represent the average of six to ten individual load–unload plots at the load value specified.
[b] Each alumina substrate was coated with four layers of amorphous SiC and "Si_3N_4/Si_2N_2O" originally applied by spin-coating of PCS and PDPS and pyrolysis at 1100 °C.
[c] This represents the measured depth of penetration but the analysis of the load–unload data works with an adjusted total penetration value which is the measured penetration depth plus a contribution made by two components: (1) a small initial penetration caused by the contact force when the indentor comes into contact with the sample and (2) a component due to the tip curvature which causes the contact diameter to be larger than measured.

4. Conclusion

In this study, it has been demonstrated that adherent, mostly crack-free ceramic coatings of black amorphous SiC can be formed on silicon, silica and alumina substrates by multiple depositions and firings of polycarbosilane layers in a nitrogen atmosphere at 1100 °C. Spin-coating of polycarbosilane led to more uniform coatings of SiC with a maximum thickness of ~ 2 μm for five layers of SiC. Dip-coating gave somewhat less uniform layers with a maximum of ~ 1 μm for four layers of SiC. Adherent, colourless coatings of amorphous "Si_3N_4/Si_2N_2O" can also be formed by heating polycarbosilane or PDPS layers applied to alumina substrates in an ammonia atmosphere at 1100 °C. SEM indicated that the PDPS-derived "Si_3N_4/Si_2N_2O" coatings were mostly crack-free, although the PCS-derived "Si_3N_4/Si_2N_2O" coatings appeared less uniform with the characteristic manifestation of embedded fibres and some craters on the surfaces of the coated substrates. X-ray photoelectron studies revealed that both the SiC and "Si_3N_4/Si_2N_2O" coatings were extensively surface oxidized. This finding was supported by Rutherford backscattering studies which also indicated significant phase mixing within the underlying multilayers comprising the bulk of the coatings. Abrasion resistance and microhardness measurements indicated that the PCS-derived SiC and PDPS-derived "Si_3N_4/Si_2N_2O" coatings on alumina were softer than would be expected for SiC and Si_3N_4.

Acknowledgements

The authors thank the New Zealand Foundation for Research, Science and Technology for the awarding of a post-doctoral fellowship to M. R. M., Mr Neville Baxter for the design of the dip-coater, and Mrs Kay Card, Superconducting Team in Industrial Research Ltd, for recording electron micrographs and carrying out EDX measurements. Presented in part at the International Ceramics Conference AUSTCERAM 92, Melbourne, Australia, August, 1992.

References

1. D. SEYFERTH, in "Synthesis of Some Organosilicon Polymers and Their Pyrolytic Conversion to Ceramics", Silicon-Based Polymer Science, A Comprehensive Resource, edited by J. M. Ziegler and F.W. Gordon Fearon, Advances in Chemistry Series, 224 (American Chemical Society, Washington, DC, 1990) p. 565.
2. B. KANNER and R. E. KING, in "New Polymer Precursors for Silicon Nitride", *ibid.*, p. 607.
3. S. YAJIMA, Y. HASEGAWA, J. HAYASHI and M. IIMURA, *J. Mater. Sci.* **13** (1978) 2569.
4. M. PEUCKERT, T. VAAHS and M. BRÜCK, *Adv. Mater.* **2** (1990) 398.
5. K. E. GONSALVES, R. YAZICI and S. HAN, *J. Mater. Sci.* **10** (1991) 834.
6. P. FAUCHAIS, A. VARDELLE and M. VARDELLE, *Ceram. Int.* **17** (1991) 367.
7. H. E. FISCHER, D. J. LARKIN and L. V. INTERRANTE, *MRS Bull.* **16** (1991) 59.
8. S. SAITO, (ed.) 'Finer Ceramics' (Elsevier, New York, 1988) pp. 169, 187, 195.
9. W. S. COBLENZ, G. H. WISEMAN, P.B. DAVIS and R. W. RICE, *Mater. Sci. Res.* **17** (1984) 271.
10. R. HEZEL, T. MEISEL and W. STREB, *J. Appl. Phys.* **56** (1984) 1756.
11. M. R. MUCALO, N. B. MILESTONE and I. W. M. BROWN, *J. Amer. Ceram. Soc.*, submitted.
12. C. R. KRÜGER and E. R. ROCHOW, *J. Polym. Sci. A* **2** (1964) 3179.
13. D. BRIGGS and M. P. SEAH, (eds) in "Practical Surface Analysis by Auger and X-ray Photoelectron Spectroscopy" (Wiley, New York, 1983) pp. 488–9.
14. L. R. DOOLITTLE, *Nucl. Instrum. Meth.* **B9** (1985) 334.
15. "RUMP Users Manual" (Computer Graphics Services, 52 Genung Circle, Ithaca, NY, 14850, USA).
16. J. S. FIELD, *Surf. Coat. Technol.* **36** (1988) 817.
17. T. J. BELL, A. BENDELI, J. S. FIELD, M. V. SWAIN and E. G. THWAITE, *Metrologia* **28** (1992/92) 463.

18. D. SEYFERTH and G. H. WISEMAN, in "Silazane Precursors to Silicon Nitride", Silicon-Based Polymer Science, A Comprehensive Resource, edited by J. M. Ziegler and F. W. Gordon Fearon, Advances in Chemistry Series, 224 (American Chemical Society, Washington, DC, 1990) p. 265.
19. K. KANAYA and S. OKAYAMA, *J. Phys. D Appl. Phys.* **5** (1972) 43.
20. J. F. LYNCH (ed.), "Engineering Property Data on Selected Ceramics", Vol. 2, "Carbides" (Metals and Ceramics Information Centre, Batelle, Columbus Laboratories, OH, 1979) p. 23.
21. R. B. ROBERTS, in "Expansivity of Silicon 20–500 °C", Thermal Expansion 6, edited by I. D. Peggs (Plenum Press, New York, 1978) p. 187.
22. R. C. WEAST (ed.), "CRC Handbook of Chemistry and Physics" (CRC Press, FL, 1985) p. F56.
23. J. F. LYNCH, G. G. RUDERER and W. H. DUCKWORTH (eds), "Engineering Property Data on Selected Ceramics", Vol. 1, "Nitrides" (Metals and Ceramics Information Centre, Batelle, Columbus Laboratories, OH, 1976) p. 1.
24. P. SCHRECK, C. VIX-GUTERL, P. EHRBURGER and J. LAMAYE, *J. Mater. Sci.* **27** (1992) 4243.
25. M. R. MUCALO and N. B. MILESTONE, *J. Amer. Ceram. Soc.*, submitted.
26. T. A. CARLSON, "Photoelectron and Auger Spectroscopy" (Plenum Press, New York, 1975) p. 349.
27. H. VINCENT, C. VINCENT, L. ODDOU and T. S. KANNAN, *J. Mater. Chem.* **2** (1992) 567.
28. J. L. LOUBET, J. M. GEORGES and G. MEILLE, in "Micro-Indentation Techniques in Materials Science and Engineering", ASTM STP889, edited by P. J. Blau and B. R. Lawn (American Society for Testing and Materials, Philadelphia, PA, 1986) p. 72.
29. W. C. OLIVER and G. M. PHARR, *J. Mater. Res.* **7** (1992) 1564.
30. R. RIEDEL, G. PASSING, H. SCHONFELDER and R. J. BROOK, *Nature* **355** (1992) 714.

Received 25 June 1993
and accepted 19 January 1994